Journal of Geophysical Research: Atmospheres

RESEARCH ARTICLE
10.1029/2018JD029206

Strong Contrast in Remote Black Carbon Aerosol Loadings Between the Atlantic and Pacific Basins

Joseph M. Katich[1,2], B. H. Samset[3], T. Paul Bui[4], M. Dollner[5], K. D. Froyd[1,2], P. Campuzano-Jost[2,6], B. A. Nault[2,6], J. C. Schroder[2,6], B. Weinzierl[5], and J. P. Schwarz[1]

[1]NOAA Earth System Research Laboratory (ESRL), Chemical Sciences Division, Boulder, CO, USA, [2]Cooperative Institute for Research in Environmental Sciences (CIRES), University of Colorado Boulder, Boulder, CO, USA, [3]CICERO Center for International Climate Research, Oslo, Norway, [4]NASA Ames Research Center, Mountain View, CA, USA, [5]Faculty of Physics, Aerosol Physics and Environmental Physics, University of Vienna (UNIVIE), Vienna, Austria, [6]Department of Chemistry, University of Colorado Boulder, Boulder, CO, USA

Abstract Measurements of black carbon (BC) aerosol mass concentration in remote air are sparse, leading to poorly constrained regions that models struggle to represent. Here we present a new data set of BC concentration over the remote Pacific and Atlantic basins from 80 N to 65°S latitude that was obtained as part of NASA's Atmospheric Tomography campaign in July/August 2016. More than 100 vertical profiles, extending from ~0.2 to 13 km altitude above mean sea level, reveal sharp contrasts in loadings between the two basins. Over the Pacific, we found average BC concentration vertical profiles to be largely consistent with seasonally matched data obtained in 2011. Substantially higher loads were observed over the Atlantic in the low to middle troposphere than in the Pacific, likely due to strong regional sources and reduced convective removal in the tropics in this basin. Atlantic and Pacific BC concentrations converge in the upper troposphere and lower stratosphere, reflecting similar high-altitude background concentrations. Comparison of the Atlantic data to the Aerosol Comparisons between Observations and Models suite of models (Phase II) reinforces previous speculation about the ensemble in the remote by quantifying an upper-troposphere model-high-bias of as much as two orders of magnitude over wide latitude bands. However, these direct BC measurements reveal Aerosol Comparisons between Observations and Models ensemble underestimation of biomass burning BC in the outflow of continental Africa by nearly a factor of 5. This high-BC loading region likely dominates BC's direct radiative effect over remote areas of the Pacific and Atlantic basins during the month of August.

Key Points:
- Black carbon loadings over the remote Atlantic are generally comparable to those over the Pacific, except at low-altitude near the equator
- AeroCom's model-ensemble average overestimates loadings, except in the lower troposphere of the equatorial Atlantic region
- The direct radiative effect of BC over the remote Pacific and Atlantic in August is likely dominated by African biomass burning outflow

Supporting Information:
- Supporting Information S1
- Figure S1

Correspondence to:
J. M. Katich,
joseph.m.katich@noaa.gov

Citation:
Katich, J. M., Samset, B. H., Bui, T. P., Dollner, M., Froyd, K. D., Campuzano-Jost, P., et al. (2018). Strong contrast in remote black carbon aerosol loadings between the Atlantic and Pacific basins. *Journal of Geophysical Research: Atmospheres*, *123*, 13,386–13,395. https://doi.org/10.1029/2018JD029206

Received 19 JUN 2018
Accepted 23 OCT 2018
Accepted article online 5 NOV 2018
Published online 4 DEC 2018

Author Contributions:
Conceptualization: Joseph M. Katich, B. H. Samset, J. P. Schwarz
Data curation: Joseph M. Katich
Formal analysis: Joseph M. Katich
Investigation: Joseph M. Katich, T. Paul Bui, M. Dollner, K. D. Froyd, P. Campuzano-Jost, B. A. Nault, J. C. Schroder, B. Weinzierl, J. P. Schwarz
Methodology: Joseph M. Katich, B. H. Samset, K. D. Froyd, P. Campuzano-Jost, B. A. Nault, J. C. Schroder, B. Weinzierl, J. P. Schwarz
Resources: B. H. Samset
Supervision: J. P. Schwarz
Visualization: Joseph M. Katich
(continued)

1. Introduction

Black carbon (BC), a byproduct of incomplete combustion, absorbs solar radiation more efficiently than any other aerosol material in the atmosphere and is a substantial contributor to global radiative forcing (Bond et al., 2013; IPCC, 2014). Further, BC aerosol has disproportionately large direct, indirect, and semidirect impacts on climate uncertainty (Carslaw et al., 2013; IPCC, 2014; Koch & Del Genio, 2010). This uncertainty is partially due to biases in model estimates of BC's global concentrations, which, in some remote regions, are strongly driven by insufficient understanding of the processes by which BC is removed from the atmosphere.

Large relative discrepancies exist between climatological model predictions of BC concentration and observations, especially far from sources and at high altitudes. Measurements from the High-performance Instrumented Airborne Platform for Environmental Research Pole-to-Pole Observations (HIPPO, Schwarz et al., 2013) as well as a collection of primarily northern hemisphere missions spanning a large longitudinal range (Schwarz et al., 2017) revealed regions with substantial vertical gradients in BC concentrations above both remote ocean and populated continental regions, and approximately uniform loadings in the upper troposphere and lower stratosphere (UTLS). These measurements deviate significantly from the average model-ensemble predictions of the Aerosol Comparisons between Observations and Models (AeroCom), demonstrating a high bias of model-generated concentrations that are at times factors of 10 too large, especially in the UTLS. Samset et al. (2014) attribute some of this bias to overestimated BC lifetime, or mean atmospheric residence time, and found that a global lifetime of less than 5 days is necessary to harmonize even the best-performing AeroCom contributors with remote aircraft data. Wang et al. (2014) calculate a tropospheric BC lifetime of 4.2 days as necessary to reconcile GEOS-Chem model performance with HIPPO

Writing - original draft: Joseph M. Katich
Writing – review & editing: Joseph M. Katich, B. H. Samset, T. Paul Bui, K. D. Froyd, P. Campuzano-Jost, B. A. Nault, J. C. Schroder, B. Weinzierl, J. P. Schwarz

observations, which was achieved by implementing more efficient wet scavenging in the model. They also note that the difference between their estimates of global top-of-atmosphere direct radiative forcing and the likes of Bond et al. (2013) is driven by estimates of BC concentration over oceans and in the free troposphere. Additionally, measured background UTLS concentrations appear to vary on month-long time scales due to nonseasonal processes, indicative of different long-term concentration states that are currently unexplained. Clearly, improved knowledge of BC concentrations over global scales is necessary to properly predict BC's effect on climate. Thus, more aircraft measurements are essential to develop tighter constraints on concentrations, especially in areas where the presence of BC is predominantly driven by transport and wet scavenging.

The data set presented here closely replicates the HIPPO sampling of BC over the Pacific and is extended to the Atlantic basin, where different processes and source regions affect BC vertical profiles. This sampling occurred as part of the first installment of NASA's Atmospheric Tomography mission (ATom, with the first installment referred to as *ATom1*). Refractory BC (rBC) concentrations were determined with a single-particle soot photometer (SP2, Droplet Measurement Technologies, Longmont, CO). Collected over a 4-week period spanning July–August 2016, ATom provides near a pole-to-pole survey of the atmosphere's gas and aerosol composition through most of the troposphere and at times into the lower stratosphere. Flight tracks of near-continuous profiling ranged from 0.2 to 13 km above mean sea level (AMSL), with latitude coverage of S65 to N80. The data offer a first opportunity to asses global-scale remote Atlantic BC loadings and to compare remote Pacific BC measurements to previous seasonally matched observations over a near-complete latitude range.

The experimental details are discussed in section 2. Section 3 presents the results including Atlantic and Pacific loadings, Pacific observations compared to seasonally resolved HIPPO data, comparisons to model results generated by the Phase II AeroCom suite (http://aerocom.met.no), and comparison of estimates of BC's direct radiative effect (DRE) over the Pacific and Atlantic basins using both ATom1 measurement and models as inputs. A summary of results with their significance and implications is provided in section 3.1.

2. Experimental Details

A NOAA SP2, flown onboard NASA's DC-8 (https://airbornescience.nasa.gov/aircraft/DC-8), was used to detect the rBC mass content of individual aerosol particles in the accumulation mode. Here we use the term rBC as recommended by Petzold et al. (2013) to refer to the specific material quantified by laser induced incandescence, the technique used by the SP2. The SP2 relies on well-established methods with reasonably well-quantified uncertainties and has been successfully deployed on aircrafts for over a decade (Schwarz et al., 2006, and many others). rBC masses are determined by relating peak incandescent signal from fullerene soot, a proxy for atmospheric BC (Baumgardner et al., 2012), to the mass of mobility diameter-selected soot via the parameterization of Gysel et al. (2011). This mass determination is independent of particle morphology (Cross et al., 2010; Moteki & Kondo, 2010; Slowik et al., 2007). rBC particle size distributions can be achieved by converting particle mass to a volume equivalent diameter, assuming a void-free density of 1.8 g/cm^3. While the lower limit of rBC detection ultimately depends on the instrument's laser intensity (Schwarz, Spackman, Gao, Perring, et al., 2010), the upper limit can be adjusted via detector gain and sampling line strategy. Here the upper limit of detection was set to cover the majority of rBC typically present within the accumulation mode (up to ~550 nm) for flights over the Pacific basin and extended to ~725 nm volume equivalent diameter over the Atlantic to assess possible contributions of larger particles to total rBC mass concentration. However, no significant contribution to mass fraction was observed above 550 nm. Mass mixing ratios (MMRs) are formulated by summing the total mass of rBC particles in a volume of ambient air and reported as ng rBC/kg air (henceforth, simply ng/kg). As is typical for SP2 determinations of ambient rBC accumulation-mode concentration, these MMRs are scaled upward by a missing-mass factor to account for undetected rBC mass. This factor is calculated via extrapolation of a lognormal fit to the rBC mass-size distributions to determine the fraction of accumulation mode mass quantified within the SP2's dynamic range. In remote environments, concentrations are typically low enough that long time scales of integration are necessary to obtain a robust size distribution, thus this correction is performed on a flight-by-flight basis (rather than a shorter time scale). On average during ATom1, the SP2 detected 91% of accumulation mode mass. The total uncertainty of MMRs calculated for 1 km bins is 30%, about half of

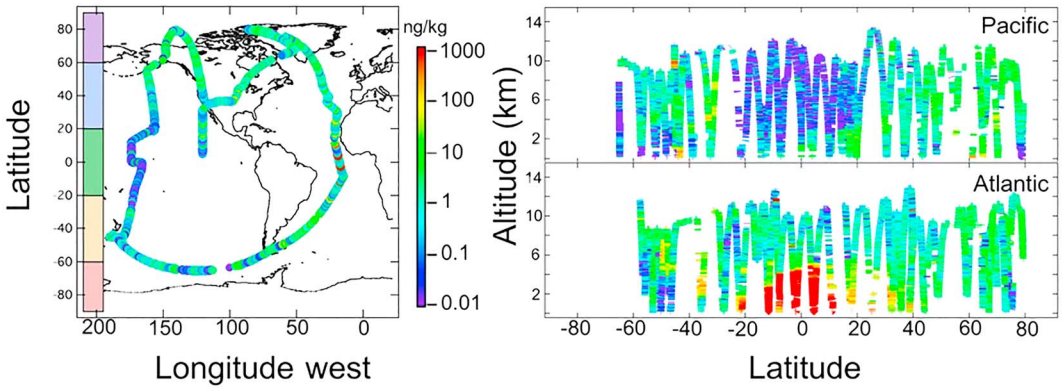

Figure 1. (left) Flight tracks (colored line) of the NASA DC-8 during the ATom1 August 2016 deployment. Colored boxes at the far-left show latitude binning for Pacific and Atlantic data. (right) Altitude versus latitude for the Pacific (top) and Atlantic (bottom), colored by black carbon mass-mixing ratio in units of ng rBC/kg of air. The color scale between the figures, which applies to all of Figure 1, represents black carbon mass mixing ratio in ng/kg.

which is associated with difference in SP2 response between the fullerene soot calibration standard and ambient rBC (Kondo et al., 2011; Laborde et al., 2012). All ATom rBC MMR data used in this analysis can be found at Katich et al. (2018), which is a subset of Wofsy et al. (2018). A complete description of the SP2 design and performance can be found in Schwarz et al. (2006).

The rBC vertical profiles exclude data collected in clouds, as impaction of ice or water crystals on the sampling inlet can generate data artifacts (Murphy et al., 2004). Cloud cuts were generated using data from a Cloud Aerosol and Precipitation Spectrometer (Droplet Measurement Technologies, Longmont, CO), with 3 s of data on each side of cloudy regions removed to account for slight timing offsets. Locally sourced pollution at take-off and landing is also excluded from the analysis (including when performing lognormal fits to size distributions). Additionally, in-flight calibrations were removed, as were any periods in which the SP2 sample flow was outside the range of 0.5–6 vccs (usually due to abrupt aircraft maneuvers). Lengthy horizontal stays at the tops of ascents were not included in the profile analysis to avoid biasing the latitude/longitude associated with a profile.

3. Observations and Interpretation

The flight path of ATom1 is shown in the left panel of Figure 1. The right panel shows 0.1 Hz data of altitude versus latitude colored by rBC MMR. The aircraft consistently ascended beyond 12 km AMSL, but did not reach above 13 km. For each ascent or descent of the aircraft, rBC MMR measurements were averaged with 1-km high altitude bins to form one profile measurement. We use five latitude ranges (N60–N90, *northern polar*; N20–N60, *northern midlatitudes*; S20–N20, *equatorial*; S60–S20, *southern midlatitudes*, S90–S60, *southern polar*) to match the averaging ranges used in earlier HIPPO analyses, and we separate analysis of the Pacific and Atlantic basins. Individual profiles within the latitude/longitude bins are averaged together with equal weighting to arrive at an average representative profile for each region. This treatment of profile averaging is the same as is followed in Schwarz, Spackman, Gao, Watts, et al. (2010) and Schwarz et al. (2013, 2017) and has the benefit of providing our best estimate of the average loading relevant to rBC direct forcing. This approach is free of bias introduced in nonuniform sampling (e.g., due to air traffic control requiring an extended level leg within a profile), and also allows estimation of variability via comparison of individual profile measurements within each region. Constituent profiles contributing to each bins' average can be found in supporting information Figures S1 and S2.

The authors recognize that the latitude bins used here, which are chosen for sake of comparison to previous Pacific data with matching latitudinal binning, are not optimally defined in terms of the influencing source regions. This is evident, for instance, in the northern midlatitudes. In this region, our profile presentation indicates a strong low-altitude contrast between the Pacific and Atlantic extending from N20 to N60. However, inspection of the rBC spatial distribution in Figure 1 reveals that the major difference only extends as far as N40 latitude. To this extent, some discretion is necessary on the readers' part when interpreting the profiles.

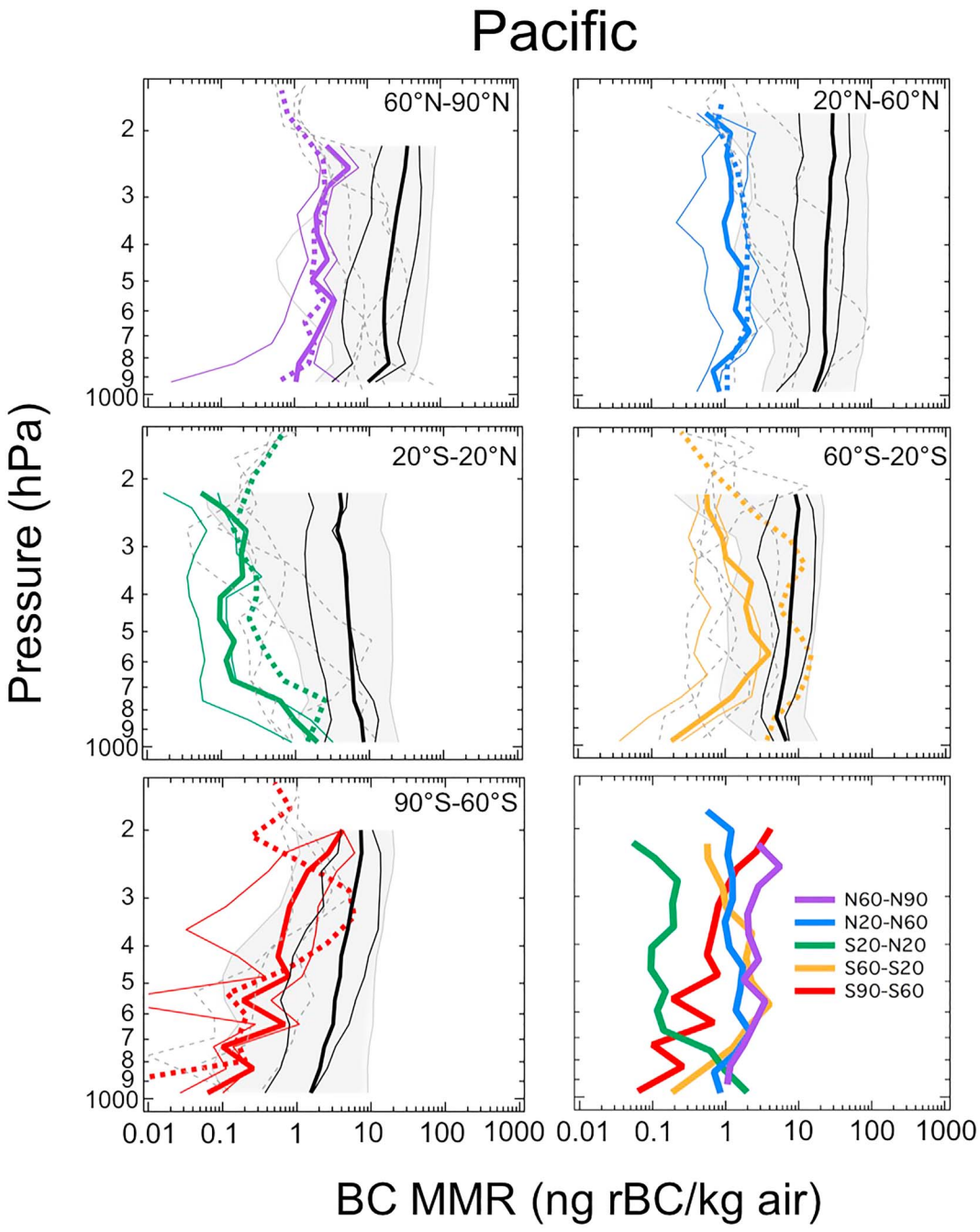

Figure 2. Pacific ATom1 rBC mass-loading vertical profiles with 1 km vertical binning. Solid thick colored line is ATom1 average profile data, with 25th and 75th percentile shown in solid thin lines of the same color. Colored dashed line is HIPPO5 (which was during the same season). Gray dashed lines are other High-performance Instrumented Airborne Platform for Environmental Research Pole-to-Pole Observations deployments for scale of seasonal variation. Thick black line is the Aerosol Comparisons between Observations and Models suite average with 25th and 75th percentile shown in the thin black line. Gray shading represents the minimum and maximum Aerosol Comparisons between Observations and Models values. The bottom right panel shows all ATom1 remote Pacific profiles. BC = black carbon; MMR = mass mixing ratio; rBC = refractory BC.

3.1. rBC Spatial Distributions

Vertical rBC MMR profiles for each region in the Pacific are shown in Figure 2. Here the solid colored line represents the average of the individual profiles in the region (individual profiles are available in supporting information). The colored dashed lines in Figure 2 represents the seasonally matched HIPPO data (HIPPO5 for this data set). Dashed gray lines represent the remaining HIPPO deployments, which provide a sense of

variations due to seasonality. Average Pacific rBC profile MMRs ranged from 0.05 to 5 ng/kg, with the lowest rBC loadings observed in the lower troposphere of the southern polar region. The highest MMRs were at high altitude near both poles and midaltitude in the southern midlatitude region, though the high-altitude polar data are relatively limited in statistics compared to the other regions explored here. The agreement between ATom1 and HIPPO5 in both the northern polar and midlatitude regions is remarkable, showing no statistically significant difference in N60–N90 and only a slight difference at midaltitude between N20 and N60. The equatorial region (S20–N20), which shows distinct evidence of convectively processed clean air in the pressure range 450–850 hPa, exhibits consistency in the two data sets at both low and high altitude, with approximately 1 standard deviation (calculated using individual profiles) lower loading at midaltitudes. This difference becomes more significant in the southern midlatitudes (S60–S20), where the ATom data are clearly statistically lower throughout the column, until an apparent convergence at the top. However, compared to the overall seasonal variation of all HIPPO data, the two average profiles are still comparable. Observations in the southern Pacific, while of poor statistical significance due to low profile count, generally reveal similar concentrations as in HIPPO, and evidence the same vertical trends now expected in the region due to high altitude transport and low altitude removal.

The comparison between ATom1 and the seasonally matched HIPPO data can be used as a test for evaluating the relationship between short-time scale remote BC measurements averaged over large areas and climatological averages. Overall, we find reasonable agreement between the two data sets. Within individual latitude bands and altitude ranges, some variability exists (lower pane of Figure S4), and the global-scale average (Figure S4, black trace) also exhibits variation, spanning an order of magnitude over the altitude range explored when all five latitude bins are included. However, this variation drops to just a factor of two when the S90–S60 bin, which has poor statistics, is excluded. Using a simple vertical-line fit to the global-scale average as an indicator of agreement, we calculate an average ATom1/HIPPO5 ratio of 1.05. Further, in all regions, the seasonal variation between HIPPO deployments is significantly larger than that between seasonally matched ATom1 and HIPPO profiles. While the degree to which ATom BC data can be considered climatologically representative is currently unknown and the subject of ongoing analyses, these findings strengthen confidence that background BC concentration profiles have long-scale climatological relevance and provides some scale for variability within the climatology.

Average Atlantic rBC profile MMRs span the range of 0.2 to 640 ng/kg and, in the lower and middle troposphere, are often substantially higher than Pacific loadings at comparable latitudes. The one obvious exception to this is the northern polar Atlantic where loadings were low and stable throughout the entire column, with the average never exceeding 2.5 ng/kg at any altitude before falling back to just below 1 ng/kg at ~190 hPa. The highest Atlantic MMRs are associated with African BB (S22–N12 latitude) and Saharan dust outflow (N16–N34 latitude) below 6 km. These enhanced loadings noticeably affect both the northern and southern midlatitude regions, though more so in the northern hemisphere. Both midlatitude regions exhibit not only substantial vertical gradients, but also latitudinal gradients at low altitude, with larger values near the tropics. For instance, the southern midlatitude region's average MMR below 1 km, at 25 ng/kg, is biased by the two most northern of the 11 measured profiles (31 and 234 ng/kg at 27S and 21S latitude, respectively). The average drops to 0.5 ng/kg when these two constituent profiles are excluded. However, as the influence of BB outflow tapers dramatically at 500 hPa, these two profiles do not bias the profile high throughout the column. Low-altitude loadings in the northern midlatitude region reveal weaker latitudinal gradients, likely due to the gradual mixing of Saharan dust outflow with northern hemisphere anthropogenic outflow.

The equatorial region itself has extremely high and relatively uniform concentrations, as high as 600 ng/kg, which are constrained to pressures higher than 600 hPa (here below ~4 km AMSL) and exhibit very little latitudinal variation. In fact, the extraordinary MMRs found here make up about 60% of the total rBC mass sampled over remote ocean during ATom1. The observed loadings are in good agreement with the measurements of Zuidema et al. (2018), who continuously monitored boundary layer rBC loadings on Ascension Island from June 2016 to October 2017 as part of the Layered Atlantic Smoke Interactions with Clouds campaign. Inspection of Layered Atlantic Smoke Interactions with Clouds data over a 5-month period (which is inclusive of the time period of ATom1) reveals that BC concentrations far from Africa's coast, which peaked at more than 1,700 ng/kg at Ascension in mid-August, regularly exceeded 100 ng/kg. These concentrations are well beyond those typically observed over remote ocean. Further, the African outflow

as viewed by ATom1 spanned roughly 30° of latitude (refer to Figure 1), with near-surface concentrations typically above 500 ng/kg and never falling below 100 ng/kg (see Figure S2). These two points lead us to postulate that our Atlantic equatorial profiles is representative of a persistent large-scale plume predominantly contained within our defined equatorial region, and not simply due to the interception of a short-lived event. Ongoing analysis of Atom 2–4 will provide valuable insight regarding this.

Between altitudes of 4 and 6 km (600 and 460 hPa), a dramatic drop-off in concentrations occurs in the equatorial region before tapering to much lower uniform loadings of about 1 ng/kg. Hybrid Single-Particle Lagrangian Integrated Trajectory back trajectories confirm that while the rBC below 4 km can be attributed almost solely to African outflow, there exists variation in the source regions above this altitude. This suggests that the air masses above this level have experienced a more diverse history, including the transport and aging processes of rBC contained within. Still, due to the abundance of rBC in the lower troposphere, it is likely that some nonnegligible fraction of the high-altitude rBC in this region is due to upward transport via deep convection. This could in part explain the ratio of middle and upper troposphere rBC in the Atlantic to the Pacific, which varies between a factor of 2 and 10.

One consistent feature of the ATom1 data set that strengthens previous conjecture is that while loadings are markedly different in several instances, all average rBC MMR profiles excepting the Pacific equatorial region ultimately converge in the UT to values between ~0.2 and 4 ng/kg. This is in agreement with the findings of the five HIPPO deployments as well as a combined global data set presented in Schwarz et al. (2017). Note that ATom1 flights did not reach altitudes at which the Pacific equatorial profile from HIPPO was seen to converged to the aforementioned levels, though the effect has been observed by other high-altitude equatorial measurements such as Spackman et al. (2011). Overall, this feature of the ATom1 data strongly supports the supposition that UTLS loadings reflect long-term and global-scale uniformity and can be used as a simple challenge for global models.

3.2. Comparison to AeroCom Model Suite Climatology

Here we compare ATom1 profiles to model predictions from the Phase II AeroCom suite (Myhre et al., 2013). Thirteen different models used emission inventories from the year 2000 and meteorology from 2006 to generate a monthly average output (here August) for rBC MMRs along the flight path. AeroCom's monthly time resolution is notably longer than the time scales over which the ATom measurements occurred within each latitude bin (typically 1–3 days). Further, the spatial resolution of grids in the AeroCom calculations is notably finer than our latitude bins (which are 10 s of degrees in latitude). Hence, some care in interpreting a comparison is needed lest transient events skew our evaluation of model performance. For this analysis, we speculate that potential errors from small-scale spatial and short-length temporal variations are negligible relative to the model biases we observe. The ATom analysis length scales are so large and measurements are made so far from sources that the potential for both spatial and temporal sampling errors is reduced (Schutgens, Gryspeerdt, et al., 2016; Schutgens, Partridge, et al., 2016). As comparison of ATom1 Pacific data to HIPPO indicates a reasonable degree of climatological representativeness, we do not expect these sampling limitations to greatly curb our ability to assess ensemble performance of AeroCom models in the Atlantic.

Shown in Figures 2 and 3 alongside the ATom1 observations are the ensemble-average profiles of all 13 models, which is interpolated to the ATom1 profile latitudes, longitudes, and altitudes. A high bias in Phase II AeroCom ensemble BC estimates over much of the remote atmosphere and at high altitudes is well established (Samset et al., 2014; Schwarz et al., 2013, 2017), and it should be noted that several of the included models have already been updated in response to HIPPO and other data for AeroCom Phase III. However, Phase II has yet to be compared to the Atlantic on a global scale. Not surprisingly, the Phase II models in each Pacific zone overestimate loadings from pole-to-pole at high altitude. It is notable that in this season (as was the case in HIPPO5), the average factor of ~10 overestimation of the models exhibits little altitude dependence (Figure S4), whereas the annual-average HIPPO measurement (Schwarz et al., 2013) agreed slightly better with the model-ensemble at low altitude. For ATom1 Pacific data, the southern polar region is the only bin that is inconsistent with both the general Pacific ATom1 and annual-average HIPPO model-to-measurement trends. Here the model ensemble overestimates the measurement by less than a factor of 2 at high altitude and more than a factor of 10 at low altitude. Note again, however, that this bin has relatively poor statistics compared to others. Overall, the Pacific ATom1 model-to-measurement ratios reinforce the HIPPO findings.

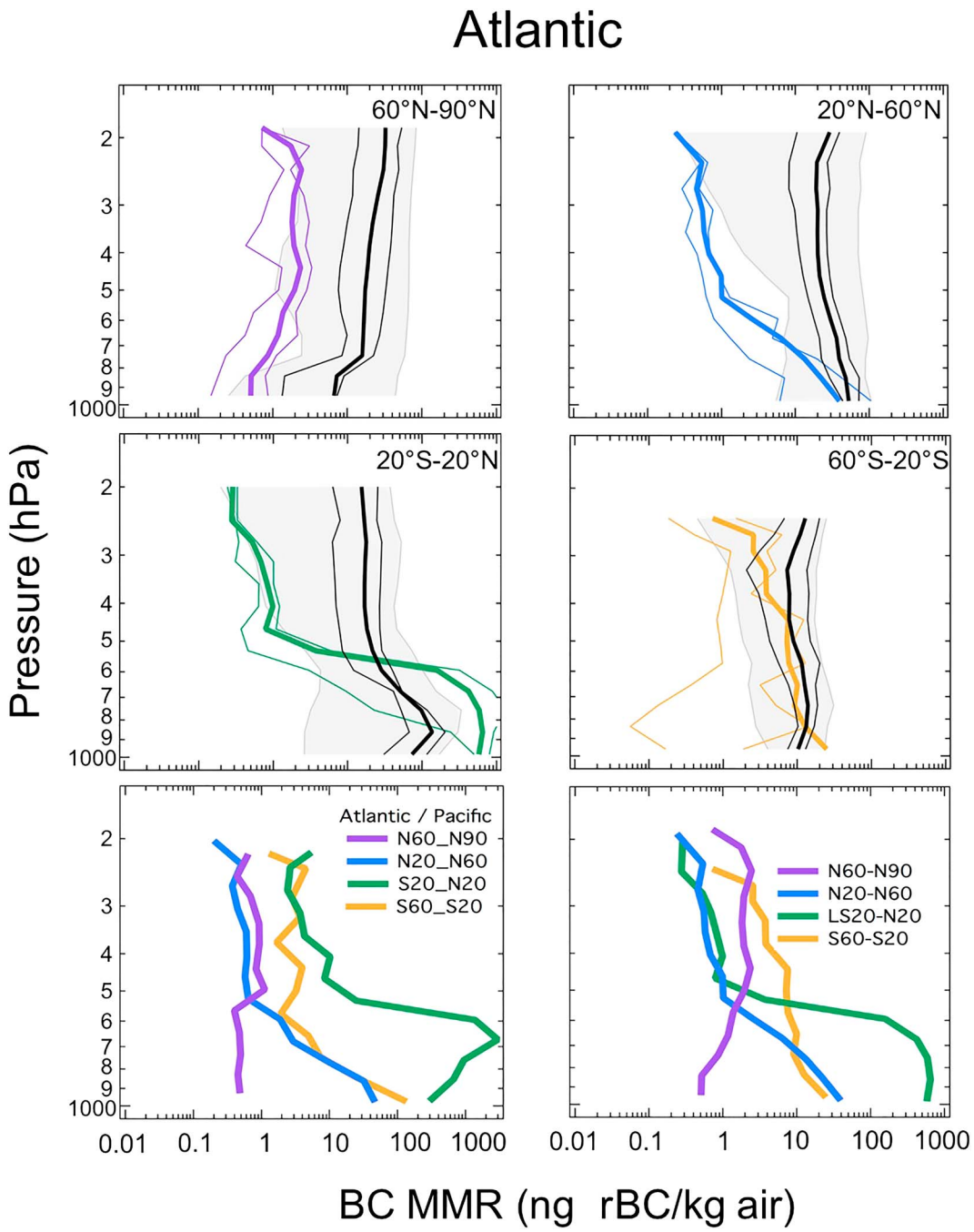

Figure 3. Atlantic ATom1 rBC mass-loading vertical profiles with 1 km vertical binning. Solid thick colored line is ATom1 average profile data, with 25th and 75th percentile shown in solid thin lines of the same color. Thick black line is Aerosol Comparisons between Observations and Models suite average with 25th and 75th percentile shown in thin black line. Gray shading represents the minimum and maximum Aerosol Comparisons between Observations and Models values. The Pacific to Atlantic ratio for each bin is shown in the lower left plot (note that there is no ratio for S90–S60, as ATom1 did not fly south of S60 in the Atlantic). The bottom right panel shows all ATom1 remote Atlantic data. BC = black carbon; MMR = mass mixing ratio; rBC = refractory BC.

The Atlantic model-to-measurement comparisons corroborate previous high-model bias conclusions at high altitude, but exhibit substantially more variation at low altitude. In areas not strongly influenced by African outflow, the model ensemble still tends to overpredict loadings to some degree across all latitudes and altitudes. In the northern polar region, this occurs by roughly an order of magnitude throughout the column. The northern midlatitude zone shows reasonable agreement at the lowest altitude before quickly diverging above the boundary layer. There is no statistical difference in southern midlatitude measurements and

Table 1
Estimates of Refractory Black Carbon's Direct Radiative Effect (in W/m^2) for Each Latitude Region Over Each Basin, Including ATom (AeroCom) Estimated DRE, an Estimate of the Fraction of Global Area, the Resulting Area-scaled DRE, and the Total Sums of the DRE That are Used to Make the Qualitative Statements in the Main Text

	A	B	C	D	E
Pacific	ATom DRE (W/m^2)	AeroCom DRE (W/m^2)	Frac Global Area	Scaled ATom DRE (W/m^2)	Scaled AeroCom DRE (W/m^2)
N60–N90	0.082	0.554	0.01	0.001	0.006
N20–N60	0.039	0.572	0.06	0.002	0.034
S20–N20	0.003	0.048	0.10	0.000(3)	0.005
S60–S20	0.024	0.084	0.07	0.002	0.006
S90–S60	0.012	0.040	0.01	0.000(1)	0.000(4)
Sum:			0.25	0.005	0.051
Atlantic	Atom DRE (W/m^2)	AeroCom DRE (W/m^2)	Frac Global Area	Scaled ATom DRE (W/m^2)	Scaled AeroCom DRE (W/m^2)
N60–N90	0.064	0.641	0.01	0.001	0.006
N20–N60	0.127	0.569	0.04	0.005	0.023
S20–N20	1.442	0.275	0.04	0.058	0.011
S60–S20	0.085	0.107	0.03	0.003	0.003
Sum:			0.12	0.067	0.043

Note. ATom = Atmospheric Tomography; DRE = direct radiative effect; AeroCom = Aerosol Comparisons between Observations and Models.

predictions throughout most of the column (~830–400 hPa, or ~1.5–8.5 km), and at the lowest measured altitude in this region (0.4 km) the measurement is a factor of 2.5 higher. As noted previously, the low-altitude measurement in this region is heavily biased by its two northern-most profiles, which are dominated by low-lying African outflow. Interestingly, inspection of individual profiles from model predictions (not shown) in this southern region show that most models generate a population of profiles that are influenced by BB, and another which is not, the average of which agrees well with our measurement. On the contrary, individual model predictions in the northern midlatitude region are consistently high above the boundary layer, which could be indicative of a difference in how the models deal with anthropogenic versus BB influence, or in their source inventories.

The equatorial region of the Atlantic is the only place along the ATom1 flightpath where measured concentrations noticeably exceeded model predictions. Enhanced rBC concentrations are predicted in the lower troposphere, presumably from African outflow, though the maximum ensemble-estimate of ~130 ng/kg is well short of the observed average concentrations of about 600 ng/kg. This underprediction stands in stark contrast to the model-high bias in most other remote areas throughout HIPPO and ATom1. Recent studies, including Kipling et al. (2013) and Wang et al. (2014) conclude that the typical model-high bias compared to HIPPO data is at least partially resolved by increasing the wet scavenging of BC. Other studies, however, indicate that regional differences in emissions, transport, and scavenging processes make it difficult to extrapolate such results to other measurement series (Lund et al., 2018). It is a reasonable starting point to assume that the low-altitude model biases in the remote equatorial Atlantic, and to some extent the midlatitude regions, are driven by incomplete emission inventories, though long-range transport and scavenging efficiencies may also contribute. Ultimately, this model overestimation, while limited to a relatively small fraction of Earth's surface area, most likely has important consequences when determining rBC's global DRE over remote ocean waters.

3.3. rBC DRE Over the Pacific and Atlantic

We estimate the DRE of rBC over the remote Pacific and Atlantic basins during the northern hemisphere summer using both ATom1 measurements and the corresponding AeroCom model predictions. This is done relying on the method presented in Samset and Myhre (2011) and Samset et al. (2014) which allows calculation of the normalized forcing of BC at different altitudes. Here we multiply each defined regions' average measured (and AeroCom modeled) BC concentration profiles (from Figures 2 and 3, which are in ng rBC/kg air) by monthly (August) regional mean profile of normalized radiative forcing (W/g BC; see Figures S5 and S6). The resulting DRE profiles are then integrated over the column to arrive at an estimate for the average column DRE in each latitude bin in the Pacific and Atlantic. These integrated values are shown for each latitude bin in Table 1, columns A and B. Those DRE numbers are then scaled by approximate *remote*

longitude ranges (Table 1, column C) such that the resulting DRE numbers (Table 1, columns D and E) roughly represent the total DRE within each latitude bin over the longitudinal span of the remote basins. The sum of Table 1, columns D and E, over each basin represent the total DRE calculated using either ATom1 or model data.

Over the entire Pacific basin, we find the DRE to be roughly an order of magnitude higher when using the model input (0.051 W/m^2) versus ATom1 input (0.005 W/m^2); a result not surprising, given the wide spread model high-bias in BC concentration. Conversely, in the Atlantic the DRE when calculated with model input (0.043 W/m^2) is just over one half of that calculated with ATom1 data (0.067 W/m^2), reflecting the significant low bias in the model in the African biomass-burning outflow. Indeed, the total sum of the DRE in the remote Atlantic (0.067 W/m^2) is more than an order of magnitude larger than in the remote Pacific (0.005 W/m^2) when using ATom1 data as input, compared to being roughly equivalent (0.051 W/m^2) for model input. Combining the Pacific and Atlantic, we estimate the sum of DRE over both basins to be quite comparable when using model input (0.094 W/m^2) versus ATom1 data (0.072 W/m^2). This finding is markedly different than previous conjecture in Schwarz et al. (2013), which suggested that model-overestimates of DRE in remote atmospheres could potentially be even higher than their concluded range of a factor of 3–11. While the DRE calculations presented here are specific to August 2016, it is possible that models underestimate the DRE over remote oceans during all portions of the year when African biomass burning is significant.

4. Conclusion

We have measured BC concentrations over remote regions of the Pacific and Atlantic basins during the first installment of NASA's ATom campaign in August of 2016. The data highlight dramatic differences in loadings between the two basins and provide valuable new constraints on BC concentrations in remote regions throughout the globe, which in most areas are dominated by long-range transport and removal. The Pacific data are generally in good agreement with seasonally matched HIPPO data, supporting the climatological relevance of background BC loading profile measurements averaged over large latitude bands. The Atlantic loadings are often higher than the Pacific, especially in lower altitude regions that are heavily influenced by outflow from Africa including biomass burning and dust source regions. The data show significant vertical gradients of rBC loadings in both the Pacific and Atlantic that converge to near-uniform (relative to the overall span of observed) concentrations of 0.2–4 ng/kg in the UTLS, which strongly supports the idea of globally uniform rBC loadings in the UTLS. Comparison of Phase II AeroCom ensemble-average BC load predictions to the expansive remote Atlantic measurements supports previous findings that concentrations are dramatically overestimated in the UTLS throughout the globe. However, model-low biases of BC loadings below 5 km in the Atlantic equatorial region likely negates any significant high AeroCom-ensemble bias in total BC DRE over remote ocean waters during peak burning seasons. Ultimately, more seasonal measurements of BC loadings in both remote regions and near sources remain necessary to further constrain the global BC burden and their effects on DRE.

Acknowledgments
The authors thank the pilots and crew of the NASA DC-8 for their role in obtaining the data. We also thank Chuck Brock, Aga Kupc, and Christina Williamson for their assistance with in-flight filter tests and time-syncing of the final data. The work presented in this manuscript is supported by the ATom investigation under National Aeronautics and Space Administration's Earth Venture program (grant NNX15AJ23G). Authors B. Weinzierl and M. Dollner acknowledge funding from the European Research Council (ERC) under the European Union's Horizon 2020 Research and Innovation Programme under grant agreement 640458 (A-LIFE). Aircraft data from the ATom mission are available at https://dx.doi.org/10.5067/Aircraft/ATom/TraceGas_Aerosol_Global_Distribution, while the data specific to this analysis can be found at Katich et al. (2018). HIPPO data are available at https://www.eol.ucar.edu/field_projects/hippo. Aerocom data can be found online at http://aerocom.met.no. The authors declare no conflicts of interest.

References

Baumgardner, D., Popovicheva, O., Allan, J., Bernardoni, V., Cao, J., Cavalli, F., et al. (2012). Soot reference materials for instrument calibration and intercomparisons: A workshop summary with recommendations. *Atmospheric Measurement Techniques*, *5*, 1869–1887. https://doi.org/10.5194/amt-5-1869-2012

Bond, T. C., Doherty, S. J., Fahey, D. W., Forster, P. M., Berntsen, T., DeAngelo, B. J., et al. (2013). Bounding the role of black carbon in the climate system: A scientific assessment. *Journal of Geophysical Research: Atmospheres*, *118*, 5380–5552. https://doi.org/10.1002/jgrd.50171

Carslaw, K. S., Lee, L. A., Reddington, C. L., Pringle, K. J., Rap, A., Forster, P. M., et al. (2013). Large contribution of natural aerosols to uncertainty in indirect forcing. *Nature*, *503*, 67–71. https://doi.org/10.1038/nature12674

Cross, E. S., Onasch, T. B., Ahern, A., Wrobel, W., Slowik, J. G., Olfert, J., et al. (2010). Soot particle studies—Instrument inter-comparison—Project overview. *Aerosol Science and Technology*, *44*, 592–611. https://doi.org/10.1080/02786826.2010.482113

Gysel, M., Laborde, M., Olfert, J. S., Subramanian, R., & Grohn, A. J. (2011). Effective density of Aquadag and fullerene soot black carbon reference materials used for SP2 calibration. *Atmospheric Measurement Techniques*, *4*, 2851–2858. https://doi.org/10.5194/amt-4-2851-2011

IPCC (2014). Climate Change 2014: Synthesis Report. In Core Writing Team, R. K. Pachauri, & L. A. Meyer (Eds.), *Contribution of working groups I, II and III to the fifth assessment report of the intergovernmental panel on climate change* (p. 151). Geneva, Switzerland: IPCC.

Katich, J. M., Schwarz, J. P., Froyd, K., Weinzierl, B., Dollner, M., Bui, T. P., et al. (2018). *ATom: Black carbon mass mixing ratios from ATom-1 flights*. Oak Ridge, Tennessee, USA: ORNL DAAC. https://doi.org/10.3334/ORNLDAAC/1618

Kipling, Z., Stier, P., Schwarz, J. P., Perring, A. E., Spackman, J. R., Mann, G. W., et al. (2013). Constraints on aerosol processes in climate models from vertically-resolved aircraft observations of black carbon. *Atmospheric Chemistry and Physics*, *13*, 5969–5986. https://doi.org/10.5194/acp-13-5969-2013

Koch, D., & Del Genio, A. D. (2010). Black carbon absorption effects on cloud cover: Review and synthesis. *Atmospheric Chemistry and Physics*, *10*, 7685–7696. https://doi.org/10.5194/acp-10-7685-2010

Kondo, Y., Sahu, L., Moteki, N., Khan, F., Takegawa, N., Liu, X., et al. (2011). Consistency and traceability of black carbon measurements made by laser-induced incandescence, thermal-optical transmittance, and filter-based photo-absorption techniques. *Aerosol Science and Technology*, *45*(2), 295–312. https://doi.org/10.1080/02786826.2010.533215

Laborde, M., Mertes, P., Zieger, P., Dommen, J., Baltensperger, U., & Gysel, M. (2012). Sensitivity of the single particle soot photometer to different black carbon types. *Atmospheric Measurement Techniques*, *5*, 1031–1043. https://doi.org/10.5194/amt-5-1031-2012

Lund, M. T., Samset, B. H., Skeie, R. B., Watson-Parris, D., Katich, J. M., Schwarz, J. P., & Weinzierl, B. (2018). Short black carbon lifetime inferred from global set of aircraft observations. *npj Climate and Atmospheric Science*. https://doi.org/10.1038/s41612-018-0040-x

Moteki, N., & Kondo, Y. (2010). Dependence of laser-induced incandescence on physical properties of black carbon aerosols: Measurements and theoretical interpretation. *Aerosol Science and Technology*, *44*(8), 663–675. https://doi.org/10.1080/02786826.2010.484450

Murphy, D. M., Cziczo, D. J., Hudson, P. K., Thomson, D. S., Wilson, J. C., Kojima, T., & Buseck, P. R. (2004). Particle generation and resuspension in aircraft inlets when flying in clouds. *Aerosol Science and Technology*, *38*(4), 401–409. https://doi.org/10.1080/02786820490443094

Myhre, G., Samset, B. H., Schulz, M., Balkanski, Y., Bauer, S., Berntsen, T. K., et al. (2013). Radiative forcing of the direct aerosol effect from AeroCom Phase II simulations. *Atmospheric Chemistry and Physics*, *13*, 1853–1877. https://doi.org/10.5194/acp-13-1853-2013

Petzold, A., Ogren, J. A., Fiebig, M., Laj, P., Li, S.-M., Baltensperger, U., et al. (2013). Recommendations for reporting "black carbon" measurements. *Atmospheric Chemistry and Physics*, *13*, 8365–8379. https://doi.org/10.5194/acp-13.8365-2103

Samset, B. H., & Myhre, G. (2011). Vertical dependence of black carbon, sulphate and biomass burning aerosol radiative forcing. *Geophysical Research Letters*, *38*, L24802. https://doi.org/10.1029/2011GL049697

Samset, B. H., Myhre, G., Herber, A., Kondo, Y., Li, S.-M., Moteki, N., et al. (2014). Modelled black carbon radiative forcing and atmospheric lifetime in AeroCom Phase II constrained by aircraft observations. *Atmospheric Chemistry and Physics*, *14*, 12,465–12,477. https://doi.org/10.5194/acp-14-12465-2014

Schutgens, N. A. J., Gryspeerdt, E., Weigum, N., Tsyro, S., Goto, D., Schulz, M., & Stier, P. (2016). Will a perfect model agree with perfect observations? The impact of spatial sampling. *Atmospheric Chemistry and Physics*, *16*, 6335–6353. https://doi.org/10.5194/acp-16-6335-2016

Schutgens, N. A. J., Partridge, D. G., & Stier, P. (2016). The importance of temporal collocation for the evaluation of aerosol models with observations. *Atmospheric Chemistry and Physics*, *16*, 1065–1079. https://doi.org/10.5194/acp-16-1065-2016

Schwarz, J. P., Gao, R. S., Fahey, D. W., Thomson, D. S., Watts, L. A., Wilson, J. C., et al. (2006). Single-particle measurements of midlatitude black carbon and light-scattering aerosols from the boundary layer to the lower stratosphere. *Journal of Geophysical Research*, *111*, D16207. https://doi.org/10.1029/2006JD007076

Schwarz, J. P., Samset, B. H., Perring, A. E., Spackman, J. R., Gao, R. S., Stier, P., et al. (2013). Global-scale seasonally resolved black carbon vertical profiles over the Pacific. *Geophysical Research Letters*, *40*, 5542–5547. https://doi.org/10.1002/2013GL057775

Schwarz, J. P., Spackman, J. R., Gao, R. S., Perring, A. E., Cross, E., Onasch, T. B., et al. (2010). The detection efficiency of the single particle soot photometer. *Aerospace Science and Technology*, *44*, 612–628. https://doi.org/10.1080/02786826.2010.481298

Schwarz, J. P., Spackman, J. R., Gao, R. S., Watts, L. A., Stier, P., Schulz, M., et al. (2010). Global-scale black carbon profiles observed in the remote atmosphere and compared to models. *Geophysical Research Letters*, *37*, L18812. https://doi.org/10.1029/2010GL044372

Schwarz, J. P., Weinzierl, B., Samset, B. H., Dollner, M., Heimerl, K., Markovic, M. Z., et al. (2017). Aircraft measurements of black carbon vertical profiles show upper tropospheric variability and stability. *Geophysical Research Letters*, *44*, 1132–1140. https://doi.org/10.1002/2016GL071241

Slowik, J. G., Cross, E. S., Han, J.-H., Davidovits, P., Onasch, T. B., Jayne, J. T., et al. (2007). An inter-comparison of instruments measuring black carbon content of soot particles. *Aerosol Science and Technology*, *41*, 295.

Spackman, J. R., Gao, R. S., Schwarz, J. P., Watts, L. A., Fahey, D. W., Pfister, L., & Bui, T. P. (2011). Seasonal variability of black carbon mass in the tropical tropopause layer. *Geophysical Research Letters*, *38*, L09803. https://doi.org/10.1029/2010GL046343

Wang, Q., Jacob, D. J., Spackman, R. S., Perring, A. E., Schwarz, J. P., Moteki, N., et al. (2014). Global budget and radiative forcing of black carbon aerosol: Constraints from pole-to-pole (HIPPO) observations across the Pacific. *Journal of Geophysical Research: Atmospheres*, *119*, 195–206. https://doi.org/10.1002/2013JD020824

Wofsy, S. C., Apel, E., Blake, D. R., Brock, C. A., Brune, W. H., Bui, T. P., et al. (2018). *ATom: Merged atmospheric chemistry, trace gases, and aerosols*. Oak Ridge, Tennessee, USA: ORNL DAAC. https://doi.org/10.3334/ORNLDAAC/1581

Zuidema, P., Sedlacek, A. J. III, Flynn, C., Springston, S., Delgadillo, R., Zhang, J., et al. (2018). The Ascension Island boundary layer in the remote Southeast Atlantic is often smoky. *Geophysical Research Letters*, *45*, 4456–4465. https://doi.org/10.1002/2017GL076926